JOURNAL OF GUIDANCE, CONTROL, AND DYNAMICS
Vol. 18, No. 6, November–December 1995

Magnetic Precession and Product-of-Inertia Nutation Damping of Bias Momentum Satellites

Hari B. Hablani*
Rockwell International Corporation, Downey, California 90241-7009

This paper is concerned with large-angle precession of Earth-pointing bias momentum satellites in circular orbits and small-angle precession in eccentric orbits. In the first part, ideal torque requirements are determined for precessing a momentum vector by a large yaw angle. It is then shown that a quasi-quarter-orbit open-loop magnetic precession is feasible only when the spacecraft rotation for Earth pointing is halted. For this circumstance, general relationships are developed to size a pitch dipole using a tilted dipole model of the geomagnetic field and quasi-quarter-orbit apart true anomalies whereat a pitch dipole reverses its polarity. The second part of the paper considers elliptic orbits. A pitch dipole sizing equation is developed for small-angle open-loop roll/yaw magnetic precession. This equation is then used for designing a closed-loop bang-bang precession scheme, working in concert with nutation damping via a roll/pitch product-of-inertia. A literal relationship is devised between the desired nutation damping coefficient (or time constant), roll/pitch product-of-inertia, and rate gain of a linear pitch controller.

I. Introduction

FOR efficient operation of Earth-pointing spacecraft, thermal radiators are placed so as to face the cold side of the orbit, and solar arrays are placed so as to face the warm side. Every few months, however, due to Earth's motion around the sun and due to Earth's oblateness, orbit planes of some spacecraft regress by nearly 180 deg, causing a transfer of the sun from one side of the orbit to the other side. This in turn exposes the radiators to the sun, and the array may begin to be occulted by the spacecraft bus. Moreover, if the solar array is fixed to the spacecraft at a constant angle with the orbit plane, it could become excessively off-normal to sun rays. To restore thermal equilibrium and adequate power generation, therefore, some Earth-pointing spacecraft are rotated about the yaw axis by 180 deg. Now consider a different scenario. For relatively loose pointing requirements, say, 0.5 deg in roll and pitch, for oceanography, Earth observation, geodesy, surveillance and reconnaissance, aeronomy, or scientific purposes, bias momentum satellites with magnetic attitude control systems have been used in the past and proposed for some future missions. Clearly, then, the 180 deg yaw rotations mentioned earlier of such spacecraft will necessitate a precession of bias momentum from one side of the orbit normal to the other. Although this may be accomplished using jets, doing so may not be in harmony with other mission requirements; the jets may perturb the spacecraft ephemeris, contaminate its surroundings and sensitive instruments, or limit its life span, propellant being irretrievable after expulsion. For this reason and for minimum cost, weight, and simplicity of the attitude control hardware/software, the yaw precession may instead be performed with electromagnets. Sizing a pitch dipole for this purpose is one objective of the paper. The 180 deg yaw precession is, of course, not required for all Earth-pointing bias momentum satellites; the satellites in equatorial orbit, for example, are unikely to require one.

At times, bias momentum spacecraft are designed to traverse elliptic orbits in order to focus on a certain zone of Earth, the atmosphere, and the magnetic or gravity field or to perform any other intended operation for a long duration over the slow portion of the orbit. A spacecraft in such orbits may experience strong, impulse-like atmospheric torque near perigee, inducing small (within 10 deg) roll/yaw errors in each pass. Hence the second objective of the paper is to size a pitch dipole for a small-angle closed-loop magnetic precession so that the spacecraft attains its nominal Earth-pointing attitude before diving again into the atmospheric pocket near perigee. The problem of small-angle precession arose, for instance, in the case of a multinational spacecraft AMPTE/IRM (active magnetospheric particle tracer explorers/ion release module) in a highly elliptic orbit, for which the electromagnet changed its polarity through time-tagged (that is, open-loop) commands.[1] The closed-loop magnetic precession studied here is executed in conjunction with active nutation damping effected through a roll/pitch product-of-inertia and momentum wheel speed modulation. The development of a suitable relationship between various parameters involved in this process is the last objective of the paper.

Magnetic precession is a classical concept; to our knowledge, however, the available literature does not furnish a relationship to determine the pitch dipole strength for a general spacecraft orbit, general orientation of geomagnetic field, desired precession angle, and the number of orbits allocated for the precession; see the companion paper (Ref. 2) for a review of the past, significant contributions. Space limitations forbid including this review here, but certainly, formal techniques such as optimal control as well as others have been used successfully to design the magnetic controllers; however, because of their elaborate and rigorous mathematical framework, these techniques are unsuitable for preliminary conceptual verification and parametric studies. Simple sizing equations are therefore desired and hence developed in this paper for just this purpose. The ideal torque required for a 180 deg yaw precession of an Earth-pointing bias momentum satellite in a circular orbit is determined in Sec. II. This ideal torque profile about the roll and yaw axes is compared with the one producible by the electromagnets interacting with the geomagnetic field. An unexpected conclusion emerges that, due to the Earth-pointing requirement during precession, it appears infeasible to generate the ideal torque profile magnetically in an open-loop fashion. Section III then formulates a magnetic yaw precession after halting the once-per-orbit rotation rate ω_0. This inertial yaw precession resembles the precession of spin-stabilized spacecraft, but the analysis presented here is general and fills a gap in the literature.

Focusing on the elliptic orbits next, Refs. 1 and 3–5 do demonstrate precession control with a given pitch dipole, but none of these studies provides a way of sizing the dipole for precessing a momentum vector by a specified linear angle. A quasi-quarter-orbit, open-loop magnetic controller for eccentric orbits is therefore formulated in Sec. IV, and a literal relationship is developed to size the pitch dipole. For an autonomous implementation of this scheme, the onboard magnetic controller of Rajaram and Goel[6] could be used. But inasmuch as they do not address damping of high-frequency

Received Nov. 4, 1993; revision received March 13, 1995; accepted for publication May 7, 1995.

*Senior Engineering Specialist, Advanced Programs, Avionics and Software Group, Space Systems Division, 12214 Lakewood Boulevard. Associate Fellow AIAA.

nutations excited inevitably, Sec. V presents a closed-loop, bang-bang, autonomous magnetic controller, working in conjunction with active nutation damping through a roll/pitch product-of-inertia and modulation of the momentum wheel speed with a proportional–integral–derivative (PID) pitch controller. The magnetic controller turns itself off judiciously when the spacecraft in the elliptic orbit reaches altitudes where the geomagnetic field is so feeble that it is strenuous to use it, provided the roll/yaw errors are also within deadband. The sizing equation developed in Sec. IV is employed to determine the required strength (ampere · meter^2) of the pitch dipole. A literal relationship is formulated between the specified nutation damping coefficient (or time constant), the roll/pitch product-of-inertia, and the rate gain of the pitch controller. The paper is finally concluded in Sec. VI.

II. Large-Angle Earth-Pointing Yaw Precession

Ideal Torque Requirement

By ideal, one means that the satellite's own angular momentum is negligible compared to the bias momentum $\boldsymbol{h}_s$ of the wheel residing in the satellite and spinning clockwise about the pitch or y_b axis. Figure 1 illustrates the ideal yaw precession $\alpha_{3c}(t)$ (t = time) of a bias momentum satellite about the nadir unit vector $\boldsymbol{c}_3$. The unit vector triad $\boldsymbol{c}_1\boldsymbol{c}_2\boldsymbol{c}_3$ is associated with the orbit frame $\mathcal{F}^c$: $x_c y_c z_c$ rotating clockwise at the rate $\omega_0(\omega_0 > 0)$ about the axis y_c (Fig. 1); the inertial angular rate $\boldsymbol{\omega}^{\mathcal{F}^c}$ of the frame $\mathcal{F}^c$, expressed in $\mathcal{F}^c$, is therefore $\boldsymbol{\omega}^{\mathcal{F}^c} = -\omega_0\boldsymbol{c}_2$. Furthermore, by definition, the ideal precession is accompanied with zero roll angle ($\alpha_1 = 0$) and zero pitch angle ($\alpha_2 = 0$) about the spacecraft-attached x_b and y_b axes, respectively. Consequently, the instantaneous angular momentum $\boldsymbol{h}_s$ of the wheel, during precession, can be expressed in the frame $\mathcal{F}^c$ as

$$\boldsymbol{h}_s(t) = h_s(-s\alpha_{3c}\boldsymbol{c}_1 + c\alpha_{3c}\boldsymbol{c}_2) \tag{1}$$

where $h_s < 0$ (clockwise about the unit vector $\boldsymbol{c}_2$ at $t = 0$); $s\cdot = \sin(\cdot)$ and $c\cdot = \cos(\cdot)$. In view of the angular rate $\boldsymbol{\omega}^{\mathcal{F}^c}$, the inertial derivative of $\boldsymbol{h}_s$ is

$$\dot{\boldsymbol{h}}_s = -h_s\dot{\alpha}_{3c}(c\alpha_{3c}\boldsymbol{c}_1 + s\alpha_{3c}\boldsymbol{c}_2) - h_s\omega_0 s\alpha_{3c}\boldsymbol{c}_3 \tag{2}$$

where $\dot{\alpha}_{3c}$ is the rate, not necessarily constant, at which the angular momentum is precessed. Here $\dot{\boldsymbol{h}}_s$ is the torque required for the specified yaw precession and, in view of Eq. (2), it has components not only in the roll pitch ($\boldsymbol{c}_1$–$\boldsymbol{c}_2$) plane but along the yaw axis $\boldsymbol{c}_3$ as well owing to the orbit rate ω_0 for Earth pointing. Additionally, Eq. (2) reveals that if, for example, a yaw precession of π radians is stipulated in three orbits (constrained by the battery storage capacity), then, on the average, $\omega_0/\dot{\alpha}_{3c} = 6$, and so the Earth-pointing requirement imposes a yaw control torque six times the average roll/pitch torque for the yaw precession. As we shall learn later, this renders an open-loop magnetic yaw precession infeasible.

In Fig. 1, the ideal (that is, $\alpha_1 = 0 = \alpha_2$) spacecraft-attached frame $\mathcal{F}^b$: $x_b y_b z_b$ is such that when $\alpha_{3c} = 0$, it coincides with the frame $\mathcal{F}^c$. In this ideal frame, the torque $\dot{\boldsymbol{h}}_s$ can be expressed as[2]

$$\dot{\boldsymbol{h}}_s^{\mathcal{F}^b} = -h_s[\dot{\alpha}_{3c} \quad 0 \quad \omega_0 s\alpha_{3c}]^T \tag{3}$$

where the superscript T means transpose. Equation (3) states that the precession torque $-h_s\dot{\alpha}_{3c}$ acts about the x_b axis, normal to both the instantaneous $\boldsymbol{h}_s$ along the y_b axis and the yaw precession axis $\boldsymbol{c}_3$, as expected. In addition, the torque $-h_s\omega_0 s\alpha_{3c}$ is required about the z_b axis for Earth-pointing of the spacecraft, as discussed above.

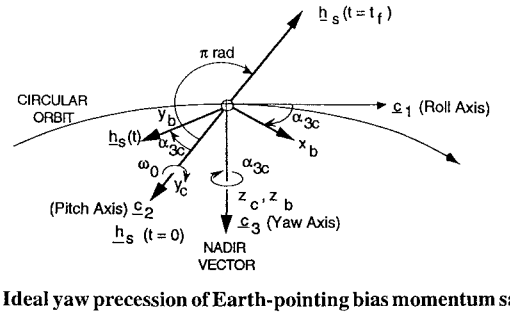

Fig. 1 Ideal yaw precession of Earth-pointing bias momentum satellite.

Yaw Precession Using Geomagnetic Field

Our next objective is to generate the torque vector (2) or (3) through the interaction of the electromagnets, residing in the spacecraft, with the geomagnetic field $\boldsymbol{B}$. Because the desired torque vector has roll (x_b-) and yaw (z_b-) components in the body-fixed frame, and because a pitch magnetic moment M_{m2} along the y_b axis generates a control torque $\boldsymbol{g}_c$ having roll and yaw components

$$\boldsymbol{g}_c^{\mathcal{F}^b} = M_{m2}[B_{b3} \quad 0 \quad -B_{b1}]^T \tag{4}$$

where $\boldsymbol{B}^{\mathcal{F}^b} = [B_{b1}\ B_{b2}\ B_{b3}]$ is the geomagnetic field in the body-fixed frame, it (the pitch dipole) appears to be an appropriate choice for producing the desired control torque.

To examine this possibility, we first note that, in the orbit frame $\mathcal{F}^c$, the field $\boldsymbol{B}$ is given by [cf. Eq. (A.12), McElvain[7]]

$$\boldsymbol{B}^{\mathcal{F}^c} = \hat{\mu}_m[s\xi_m c(\omega_0 t - \eta_m),\ -c\xi_m,\ 2s\xi_m s(\omega_0 t - \eta_m)]^T \tag{5}$$

where $\hat{\mu}_m = \mu_m/r^3$, μ_m = Earth's dipole strength (7.943×10^{15} Wb.m), r = radius of the circular orbit; the angle ξ_m is the instantaneous inclination of the orbit plane with the geomagnetic equator, and the angle η_m is the angle in the orbit plane from the instantaneous ascending node of the orbit relative to Earth's equator to the instantaneous ascending node of the orbit relative to the geomagnetic equator.[7] Because of rotation of the magnetic field with Earth and because of nodal regression, the angles ξ_m and η_m vary slowly with time and, in addition, they depend on the orbit inclination i and the angle γ_m (=11.44 deg) between Earth's magnetic dipole and the geographic north pole.[2,7]

Knowing the field $\boldsymbol{B}$ in the orbit frame $\mathcal{F}^c$, it can now be written in the ideal, precessing body frame $\mathcal{F}^b$, wherefrom the components B_{b1} and B_{b3} are placed in Eq. (4), yielding

$$\boldsymbol{g}_c^{\mathcal{F}^b} = M_{m2}\hat{\mu}_m \begin{bmatrix} 2s\xi_m s(\omega_0 t - \eta_m) \\ 0 \\ s\alpha_{3c}c\xi_m - c\alpha_{3c}s\xi_m c(\omega_0 t - \eta_m) \end{bmatrix} \tag{6}$$

Pondering over the available control torque (6) and the desired precession torque (3), we arrive at the disappointing conclusion that, whereas the desired $\boldsymbol{b}_1$ and $\boldsymbol{b}_3$ torque components in Eq. (3) are independent, the two producible components in Eq. (6) are unfortunately not. Indeed, when we modulate the magnetic momentum M_{m2} to generate the roll torque $-h_s\dot{\alpha}_{3c}$ (greater than zero, for $h_s < 0$ and $\dot{\alpha}_{3c} > 0$), the yaw component in Eq. (6) varies arbitrarily, irreverent to the desired profile $-h_s\omega_0 \sin\alpha_{3c}$. Worse yet, we fail to find any open-loop combination of modulation of the roll, pitch, and yaw dipoles, which would yield, even approximately, the three torque components in Eq. (3), including the zero pitch torque component. Consequently, it appears that the Earth-pointing requirement of the spacecraft during the yaw precession should be abandoned and an inertial precession should be considered instead. The Earth-pointing precession is possible by employing the reference maneuver scheme of Ref. 8, linear or bang-bang closed-loop orbit-averaged momentum removal schemes of Ref. 9, or the switching controller of Ref. 3, but such designs are beyond the intended scope of this paper and, besides, they will not yield a sizing equation for the pitch dipole; hence we proceed to formulate an inertial precession in the next section.

III. Inertial Yaw Precession

We now introduce a nonrotating orbit frame $\mathcal{F}^{c'}$: $x_c' y_c' z_c'$ aligned with the frame $\mathcal{F}^c$ at $\omega_0 t = 0$—the ascending node of the orbit. (Its relationship with the standard quasi-inertial frame lbn at the ascending node is obvious: $\boldsymbol{l} = -\boldsymbol{c}_3'$, $\boldsymbol{b} = \boldsymbol{c}_1'$, $\boldsymbol{n} = -\boldsymbol{c}_2'$, where the unit vectors $\boldsymbol{c}_1'$, $\boldsymbol{c}_2'$, and $\boldsymbol{c}_3'$ are along the axes x_c', y_c', and z_c', respectively, and the unit vectors $\boldsymbol{l}$, $\boldsymbol{b}$, $\boldsymbol{n}$ are defined in Sec. IV and Fig. 4.) We now redefine the ideal spacecraft-attached body frame $\mathcal{F}^b$ by aligning it initially with the frame $\mathcal{F}^{c'}$ and precessing it about the quasi-inertial axis z_c' (opposite to the ascending node line $\boldsymbol{l}$) and not rotating it about the axis y_c', y_c, or y_b for Earth pointing. This implies that the spacecraft's Earth-pointing rotation ω_0 is halted at the ascending node before commencing the precession about the yaw axis (z_b or z_c') at a certain switching true anomaly determined below.

Table 1 Parameters for inertial yaw precession of a bias momentum satellite

Roll, pitch, yaw moments of inertia	I_1, I_2, I_3	75.72, 47.45, 51.09 kg · m^2
Magnetic field at spacecraft altitude 797 km	$\hat{\mu}_m$	215 mG
Geomagnetic field dipole angle (tilt angle)	γ_m	11.44 deg
Spacecraft orbit radius and inclination	r, i	7175.14 km (797 km altitude), 108 deg
Orbit rate	ω_0	0.00104 rad/s (0.1654×10^{-3} Hz)
Orbit period	τ_0	100.76 min
Pitch bias momentum	h_s	−4.067 N · m · s
Precession angle	α_{3p}	π radians
Number of orbits for precession	N	3 (302 min)
Nutation frequency and period	$\Omega_n = \lvert h_s \rvert / \sqrt{I_1 I_3}$	0.0654 rad/s (0.0104 Hz), 96 s

Now, the torque required for the precession about the inertial axis z_c' is obtained from Eq. (2) or Eq. (3) by substituting $\omega_0 = 0$ and replacing the frame $\mathcal{F}^c$ with $\mathcal{F}^{c'}$:

$$\dot{\boldsymbol{h}}_s^{\mathcal{F}^{c'}} = -h_s \dot{\alpha}_{3c} [c\alpha_{3c} \quad s\alpha_{3c} \quad 0]^T \tag{7}$$

$$\dot{\boldsymbol{h}}_s^{\mathcal{F}^b} = -h_s \dot{\alpha}_{3c} [1 \quad 0 \quad 0]^T \tag{8}$$

On the other hand, the available, ideal ($\alpha_1 = 0 = \alpha_2$) control torque produced by a pitch dipole in the non-Earth-pointing frame $\mathcal{F}^b$ is[2]

$$\boldsymbol{g}_c^{\mathcal{F}^b} = M_{m2} \hat{\mu}_m \begin{bmatrix} \frac{1}{2} s\xi_m (-s\eta_m + 3s\theta_{m2}) \\ 0 \\ \frac{1}{2} s\xi_m c\alpha_{3c} (c\eta_m - 3c\theta_{m2}) + s\alpha_{3c} c\xi_m \end{bmatrix} \tag{9}$$

where the angle θ_{m2} varies at twice the orbit frequency: $\theta_{m2} = 2\omega_0 t - \eta_m$. As a clarification, note that, since the frame $\mathcal{F}^{c'}$, or now the body-fixed frame $\mathcal{F}^b$, does not rotate to maintain Earth pointing, it may be misleading to call the angles $\alpha_1, \alpha_2, \alpha_3$, respectively, roll, pitch, and yaw, but we continue to do so for simplicity. Moreover, the precession considered here is not general; it is restricted to that about the z_c' axis only.

From the desired equality of the roll components in Eqs. (8) and (9), we infer that the sign of the dipole M_{m2} must be reversed when the factor $[-\sin\eta_m + 3\sin(2\omega_0 t - \eta_m)]$ changes its sign [also see Eq. (8) and Fig. 3, Shigehara,[3] and Eq. (5), Rajaram and Goel[6]]. From the multiple solutions of the equation $3\sin(2\omega_0 t - \eta_m) = \sin\eta_m$, the first two switching instants t_1 and t_2 are

$$\omega_0 t_1 \triangleq \eta_1 = \tfrac{1}{2}(\eta_m + \eta_m^*) \tag{10}$$

$$\omega_0 t_2 \triangleq \eta_2 = \tfrac{1}{2}(\pi + \eta_m - \eta_m^*) \tag{11}$$

where

$$\eta_m^* \triangleq \sin^{-1}\left(\tfrac{1}{3} s\eta_m\right) \tag{12}$$

Clearly, the gap $(\eta_2 - \eta_1)$ is not a quarter orbit; rather,

$$\eta_2 - \eta_1 = \tfrac{1}{2}\pi - \eta_m^* \tag{13}$$

η_m^* being the deviation from the quarter-orbit switching. From the periodicity of the function $\sin(2\omega_0 t - \eta_m)$, the following third and fourth switching angles are also arrived at:

$$\omega_0 t_3 \triangleq \eta_3 = \pi + \eta_1 \tag{14}$$

$$\omega_0 t_4 \triangleq \eta_4 = \pi + \eta_2 \tag{15}$$

where the gap $(\eta_3 - \eta_2)$, in contrast with the gap $(\eta_2 - \eta_1)$, is

$$\eta_3 - \eta_2 = \tfrac{1}{2}\pi + \eta_m^* \tag{16}$$

Comparing Eq. (13) with Eq. (16), we conclude that the two consecutive polarities of the dipole M_{m2} are of unequal duration, although $\eta_3 - \eta_1 = \pi = \eta_4 - \eta_2$. The fifth switching instant, wherefrom the modulation of M_{m2} repeats itself, occurs at $\eta_1 + 2\pi$.

We will now determine the strength of the dipole M_{m2} required for a given yaw precession angle α_{3p} in N orbits. Since the roll torques

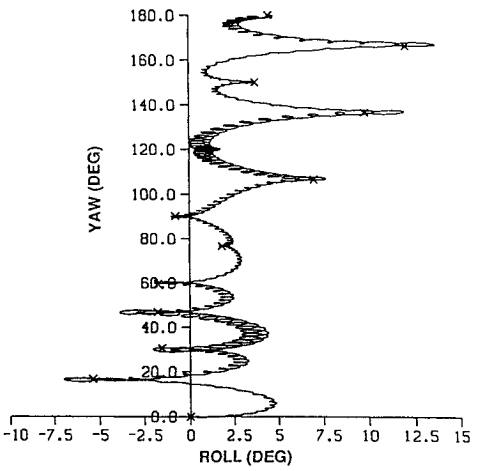

Fig. 2 180-deg inertial yaw maneuver, accompanying roll motion, and nutations.

from Eqs. (8) and (9) are equal, and since $-h_s\dot{\alpha}_{3c} > 0$, the instants of reversing the pitch dipole polarity during the yaw precession are obtained from

$$M_{m2} = |M_{m2}| \operatorname{sgn}[s\xi_m(-s\eta_m + 3s\theta_{m2})] \tag{17}$$

The precession rate $\dot{\alpha}_{3c}$ and the precession angle $\Delta\alpha_{3c}$ over one-half orbit are then found to be

$$\dot{\alpha}_{3c} = \hat{\mu}_m |M_{m2}| \, |s\xi_m(-s\eta_m + 3s\theta_{m2})| / (-2h_s) \tag{18}$$

$$\Delta\alpha_{3c} = \hat{\mu}_m |M_{m2}| \, |s\xi_m| (\eta_m^* s\eta_m + 3c\eta_m^*) / (-h_s\omega_0) \tag{19}$$

Compared with Eq. (22) of Shigehara[3] or Eq. (9) of Rajaram and Goel,[6] Eq. (19) is general. Since N orbits have $2N$ halves, the total precession angle α_{3p} will be

$$\alpha_{3p} = 2N\Delta\alpha_{3c} \tag{20}$$

which yields the following magnetic dipole strength for the yaw precession angle α_{3p} in N orbits:

$$|M_{m2}| = -h_s\omega_0\alpha_{3p} / [2N\hat{\mu}_m |\sin\xi_m| (\eta_m^* \sin\eta_m + 3\cos\eta_m^*)] \tag{21}$$

For an untilted geomagnetic field, $\eta_m = 0 = \eta_m^*$ and $\xi_m = i$, and Eq. (21) then reduces to

$$|M_{m2}| = -h_s\omega_0\alpha_{3p} / (6N\hat{\mu}_m \sin i) = -h_s\omega_0\Delta\alpha_{3c} / (3\hat{\mu}_m \sin i) \tag{22}$$

which is the same as Eq. (14) (Shigehara[3]) after resolving notational differences. For further details and illustration of Eq. (21), see Ref. 2.

For the parameters listed in Table 1, Fig. 2 illustrates an inertial yaw precession of π radians vs the accompanying roll motion in the absence of any disturbance torque over three 100-min orbits. The orientation of the magnetic field is such that the deviation angle η_m^* is maximum: $\eta_{m,\max}^* \approx \frac{1}{3}\gamma_m = 3.8$ deg for $i = 108$ deg. Although Eq. (9) furnishes the ideal magnetic torque in the spacecraft frame, the actual roll and yaw torque components for the instantaneous attitude of the spacecraft are used in the dynamics simulation. Both these components are displayed in Fig. 3. The extraneous yaw torque produces as large as 15 deg of wobbly roll motion seen in Fig. 2.

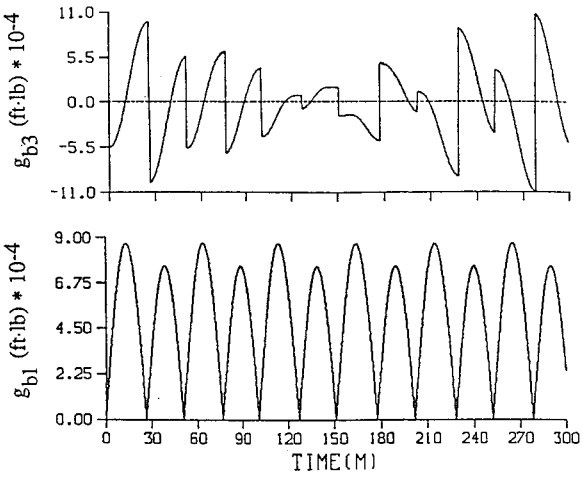

Fig. 3 Roll torque g_{b1} for inertial yaw precession and accompanying yaw torque g_{b3}.

The high-frequency, low-amplitude loops in the roll/yaw angles are nutations of the spacecraft's momentum axis (y axis). These do not grow to threaten the precession because the pitch dipole switches its polarity open loop and, insofar as nutation phase angle is concerned, randomly, without sensing the attitude and rates, every 24 or 26 min, much larger than the nutation period of 1.6 min. At the end of three orbits, although the pitch axis is precessed by 180 deg about the yaw axis, there are residual roll angle of nearly 5 deg and high-frequency nutations. They can both be eliminated by a linear magnetic controller designed in Ref. 10. As shown in Fig. 3, the roll torque g_{b1}, bringing about the precession, is a rectified sinusoid with two different peaks and durations, produced by a pitch magnetic moment of 35 A · m^2 [calculated by using Eq. (21)], changing its polarity quasiquarterly. The yaw torque g_{b3}, on the other hand, is largely mutually canceling and leaves the above-mentioned small roll error at the end.

IV. Small-Angle Open-Loop Precession in Elliptic Orbit

Figure 4 depicts the coordinate frames required for the formulation of the problem at hand. The unit vectors $\boldsymbol{l}, \boldsymbol{b}, \boldsymbol{n}$ constitute the standard lbn frame, $\mathcal{F}^{lbn}$, with $\boldsymbol{l}$ along the ascending node line, $\boldsymbol{b}$ normal to $\boldsymbol{l}$ in the orbit plane, making an acute angle with the velocity vector, and the orbit normal $\boldsymbol{n} = \boldsymbol{l} \times \boldsymbol{b}$. The rotating orbit frame $\mathcal{F}^o$: $\boldsymbol{o}_1\boldsymbol{o}_2\boldsymbol{o}_3$ is defined such that when the true anomaly η measured from the ascending node line $\boldsymbol{l}$ is zero, $\boldsymbol{o}_1 = \boldsymbol{b}$, $\boldsymbol{o}_2 = -\boldsymbol{n}$, and $\boldsymbol{o}_3 = -\boldsymbol{l}$. The frames $\mathcal{F}^c$ and $\mathcal{F}^{c'}$ introduced earlier in Sec. III are not used here because they are defined for circular orbits, for which $\mathcal{F}^o = \mathcal{F}^c$. The small yaw angle α_3 about the nadir vector $\boldsymbol{o}_3$ and the roll angle α_1 about the unit vector $\boldsymbol{o}_1$ (when $\alpha_3 = 0$) lead to the spacecraft-fixed unit vector triad $\boldsymbol{b}_1\boldsymbol{b}_2\boldsymbol{b}_3$. The radial vector $\boldsymbol{l}'$ of the frame $\boldsymbol{l}'\boldsymbol{b}'\boldsymbol{n}$ (Fig. 4) subtends an angle η_l with $\boldsymbol{l}$ and its importance will be apparent shortly. The true anomaly measured from $\boldsymbol{l}'$ is denoted ν: $\nu \triangleq \eta - \eta_l$.

Excess Angular Momentum

Nominally, the angular momentum $\boldsymbol{h}_s$ of the wheel equals $h_s\boldsymbol{o}_2 (h_s < 0)$. In the presence of roll and yaw angles, however, $\boldsymbol{h}_s$ is aligned with the instantaneous pitch axis $\boldsymbol{b}_2$ (Fig. 4), and therefore, ignoring nutations, $\boldsymbol{h}_s$ can be written in the orbit frame $\mathcal{F}^o$ as

$$\boldsymbol{h}_s^{\mathcal{F}^o} = h_s[-\alpha_3 \quad 1 \quad \alpha_1]^T \tag{23}$$

where $\boldsymbol{h}_s = h_s\boldsymbol{b}_2$ ($h_s < 0$). Because the orbit frame is rotating, the vector $\boldsymbol{h}_s$ in Eq. (23) is not in a convenient form for developing a magnetic control policy. It is therefore expressed below (as is customary) in the quasi-inertial frame $\mathcal{F}^{lbn}$,

$$\boldsymbol{h}_s^{\mathcal{F}^{lbn}} = -h_s[A_\alpha c(\mu_\alpha + \eta) \quad A_\alpha s(\mu_\alpha + \eta) \quad 1] \tag{24}$$

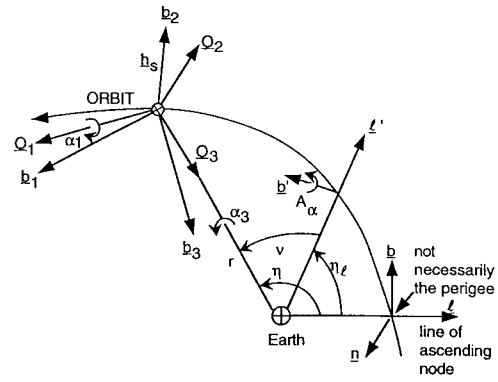

Fig. 4 Coordinate frames for bias momentum Earth-pointing satellite in elliptic orbit.

where A_α is the amplitude and μ_α the phase of the deviation of the momentum vector from its intended position $-h_s\boldsymbol{n}$ in the inertial frame:

$$A_\alpha \triangleq (\alpha_1^2 + \alpha_3^2)^{\frac{1}{2}} \qquad \mu_\alpha \triangleq \tan^{-1}(\alpha_3/\alpha_1) \tag{25}$$

Clearly, A_α is the angle to reduce to zero using a pitch dipole. The control policy for doing so can be devised with ease if $\boldsymbol{h}_s$ is now expressed in that quasi-inertial frame $\mathcal{F}^{l'b'n}$ in which, at time $t = 0$, the resultant of the $\boldsymbol{l}$ and $\boldsymbol{b}$ components of $\boldsymbol{h}_s$ is aligned with either the $\boldsymbol{l}'$ or $\boldsymbol{b}'$ unit vector in the orbit plane. It can be shown that, in the frame $\mathcal{F}^{l'b'n}$, $\boldsymbol{h}_s$ is

$$\boldsymbol{h}_s^{\mathcal{F}^{l'b'n}} = -h_s[A_\alpha c(\mu_\alpha + \eta - \eta_l), \; A_\alpha s(\mu_\alpha + \eta - \eta_l), \; 1] \tag{26}$$

At time $t = 0$, the roll and yaw angles are denoted α_{10} and α_{30} and the true anomaly η_0. Therefore, to lay the initial, undesired component of the angular momentum entirely along the unit vector, say, $\boldsymbol{l}'$, the angle η_l must be

$$\eta_l \triangleq \mu_{\alpha 0} + \eta_0 \tag{27}$$

where $\mu_{\alpha 0} \triangleq \mu_\alpha(t = 0)$. Then, the excess angular momentum at $t = 0$ is $-h_s A_{\alpha 0}\boldsymbol{l}' (A_{\alpha 0} = A_\alpha$ at $t = 0)$. Of course, instead of Eq. (27), the angle η_l could be defined such that the undesired component of the initial angular momentum is along the unit vector $\boldsymbol{b}'$, not $\boldsymbol{l}'$.

Sign Reversal Instants of Pitch Dipole

Because the initial excess angular momentum is situated entirely along $\boldsymbol{l}'$, it is helpful to express the magnetic control torque $\boldsymbol{g}_c$ also in the frame $\mathcal{F}^{l'b'n}$. Using the definition of ν ($=\eta - \eta_l$) and the analogous definition $\nu_m \triangleq \eta_m - \eta_l$, the torque produced by a pitch electromagnet of strength M_{m2} in the frame $\mathcal{F}^{l'b'n}$ is found to be[2]

$$\boldsymbol{g}_c^{\mathcal{F}^{l'b'n}} = (\mu_m/2r^3)M_{m2}s\xi_m[-c\nu_m + 3c(2\nu - \nu_m),$$
$$-s\nu_m + 3s(2\nu - \nu_m), \; 0]^T \tag{28}$$

where r is now the instantaneous radial distance of the spacecraft from Earth's mass center. To annihilate the excess momentum $-h_s A_{\alpha 0}\boldsymbol{l}'$, the angular momentum desired from the magnetic torque is $h_s A_{\alpha 0}\boldsymbol{l}'$. Therefore, the sign of M_{m2} must be such that the $\boldsymbol{l}'$ component of $\boldsymbol{g}_c$ in Eq. (28), denoted $g_{l'}$, obeys the following condition at all times until the amplitude A_α diminishes to zero:

$$\operatorname{sgn}\{M_{m2} \sin\xi_m[-\cos\nu_m + 3\cos(2\nu - \nu_m)]\} = \operatorname{sgn}(h_s A_\alpha) \tag{29}$$

Clearly, the polarity of the pitch dipole M_{m2} must be reversed when the sign of the factor $[\cdot]$ in Eq. (29) reverses; these switching instants are derived from

$$3\cos(2\nu - \nu_m) = \cos\nu_m \tag{30}$$

Also, one can just as easily arrive at the condition $3\sin(2\nu - \nu_m) = \sin\nu_m$, analogous to that in Sec. III instead of Eq. (30), by defining a unit vector $\boldsymbol{b}'$, instead of $\boldsymbol{l}'$, parallel to the given excess angular

Table 2 Parameters for small-angle precession of bias momentum spacecraft in elliptic orbit

Wheel angular momentum h_s	-67.79 N · m · s
Altitude at perigee and apogee	120 and 6000 km, respectively
Orbit eccentricity e	0.3115
Mean orbit rate ω_0 and period τ_0	0.0006885 rad/s and 152.086 min, respectively
Orbit inclination i	95 deg
True anomaly η_p at perigee	0 deg
Geomagnetic field parameters η_m, ξ_m	-11.44, 94.9 deg, respectively
Initial conditions: roll α_{10} and yaw α_{30}	-6.0, 0 deg, respectively
$\mu_{\alpha 0}$ and true anomaly η_0	180, 0 deg, respectively
η_l, ν_m, $\eta_m^\dagger$	180, 168.56, 109.07 deg, respectively
True anomalies at sign reversals: η_1, η_2, η_3, η_4	138.8, 209.74, 318.81, 29.74 deg, respectively

momentum. In any event, for $t > 0$, the first switching point $\nu \triangleq \nu_1$ obtained from Eq. (30) is

$$\nu_1 = \tfrac{1}{2}(\nu_m + \eta_m^\dagger) \tag{31}$$

where

$$\eta_m^\dagger = \cos^{-1}\left(\tfrac{1}{3}c\nu_m\right) \tag{32}$$

The definitions of ν_1 and $\eta_m^\dagger$ are analogous to the earlier definitions (10) and (12) for large-angle yaw precession. The remaining three switching instants are determined from the multiple solutions of Eq. (30), arriving at

$$\nu_2 = \nu_1 + (\pi - \eta_m^\dagger) = \pi + \tfrac{1}{2}(\nu_m - \eta_m^\dagger) \tag{33}$$

$$\nu_3 = \nu_1 + \pi \tag{34}$$

$$\nu_4 = \nu_3 + (\pi - \eta_m^\dagger) \tag{35}$$

Thus, as in the previous section, while the alternate switching points are one-half orbit apart ($\nu_3 - \nu_1 = \pi = \nu_4 - \nu_2$), the consecutive switching points are not necessarily one-quarter orbit apart unless $\nu_m = \frac{1}{2}\pi$ and then $\eta_m^\dagger = \frac{1}{2}\pi$.

Determination of Pitch Dipole Strength

Next we integrate the l' component of the magnetic torque, $g_{l'}$, from Eq. (28). Note that for a few orbit periods of magnetic control, $\mathcal{F}^{l'b'n}$ can be regarded as inertial, and so the straightforward integration of $g_{l'}$ is legitimate. The radius r and the angle ν in Eq. (28) are both time varying. To eliminate the time dependence of r, let $\bar{M}_{m2}$ be the mean pitch dipole strength, yet to be determined, and let the instantaneous magnitude of M_{m2} be

$$|M_{m2}| = r^3 \bar{M}_{m2}/a^3 \tag{36}$$

where a is the semimajor axis of the elliptic orbit. This scheme of varying the strength of a pitch dipole in proportion to r^3 and using it over the entire orbit is not always acceptable, because for highly elliptic orbits it may impose an impractical pitch dipole strength near apogee. This limitation is removed in the next section, however. Proceeding with the modulation scheme (36) for now, $g_{l'}$ transforms to

$$g_{l'} = \left(\mu_m/2a^3\right)\mathrm{sgn}(M_{m2})\bar{M}_{m2}\sin\xi_m[-\cos\nu_m + 3\cos(2\nu - \nu_m)] \tag{37}$$

where $\mathrm{sgn}(M_{m2})$ is governed by the condition (29). Integrating the factor $[\cdot]$ in Eq. (37) over the entire orbit, accounting for the sign reversals of the dipole M_{m2} at the switching anomalies $\nu_1, \ldots, \nu_4$, and then equating the accrued momentum to the desired momentum $h_s A_{\alpha 0} l'$, we obtain[2]

$$\pm 3\hat{\mu}_m \bar{M}_{m2}\sin\xi_m[(2\eta_m^\dagger - \pi)\cos\eta_m^\dagger - 2\sin\eta_m^\dagger + 3e^2\cos\hat{\eta}(\pi + \sin 2\eta_m^\dagger - 2\eta_m^\dagger)/4] = h_s\omega_0 A_{\alpha 0} \tag{38}$$

where $\hat{\mu}_m = \mu_m/a^3$, replacing the earlier definition of $\hat{\mu}_m$; $\omega_0 =$ mean orbit rate, $\hat{\eta} = \eta_m + \eta_l - 2\eta_p$, $\eta_p =$ true anomaly of the perigee measured from the ascending node line, and $e =$ orbit eccentricity. From the $\pm$ in Eq. (38), that sign is retained, which renders the two sides compatible.

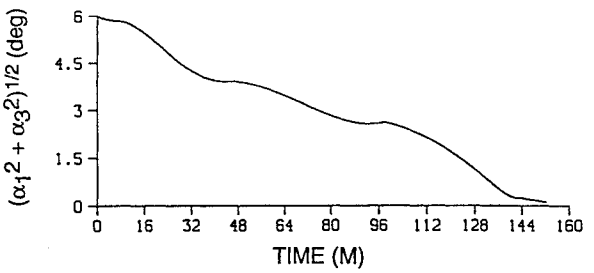

Fig. 5 Magnetic precession of momentum vector: $(\alpha_1^2+\alpha_3^2)^{1/2}$ vs time.

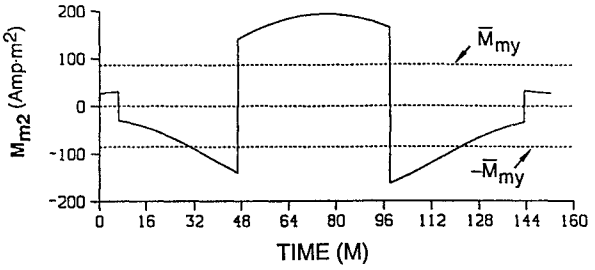

Fig. 6 Quasi-quarter-orbit sign reversal and pitch dipole strength variation over one orbit.

Illustration

Consider a bias momentum spacecraft in an elliptic orbit now. Various parameters involved, including the switching true anomalies, are furnished in Table 2. The performance of this magnetic controller is illustrated in Figs. 5 and 6, obtained by integrating two first-order momentum equations about the inertially fixed axes l' and b' under only the magnetic torque $g_{l'}$, Eq. (37), and no disturbance torque. The instantaneous true anomaly $\eta(t)$ is obtained by integrating the rate $\dot{\eta}$ for the elliptic orbit.

Figure 5 illustrates the precession of the momentum vector from an initial roll error of -6 deg to zero in one orbit period. The precession is accomplished by reversing the pitch dipole's polarity according to the law (29) at the true anomalies η_i recorded in Table 2. Instead of one-quarter orbit, the reversal takes place after 70.94 and 109.06 deg, a deviation of 19.06 deg from 90 deg (cf. Ref. 6). The open-loop precession in Fig. 5 for an elliptic orbit resembles the closed-loop precession in Fig. 3 (Ref. 6) for spin-stabilized spacecraft in a circular orbit. The polarity reversal and the variation of the pitch dipole strength are shown in Fig. 6, where the maximum required strength is found to be nearly 200 A · m^2, whereas the average strength $\bar{M}_{m2} = 85.85$ A · m^2.

The drawbacks of the above scheme are considerable, however: It is open-loop, so it may not be effective under disturbances; the dipole strength varies in proportion to r^3, so a pitch dipole of inordinate strength and hence that is costly and weighty may be required for highly elliptic orbits to utilize the weak magnetic field near apogee, and spacecraft nutations are ignored. Moreover, the scheme does not profit from the dipole's full strength near perigee where a strong magnetic field is available anyway. Hence, a more practical and efficient control scheme without these shortcomings is desired. Since a linear magnetic controller with constant gains for a circular orbit[10]

does not suit an elliptic orbit, a closed-loop bang-bang scheme along with an active nutation damper recommends itself for consideration.

V. Closed-Loop Bang-Bang Magnetic Precession and Active Nutation Damping

Although bang-bang magnetic momentum removal schemes have been used frequently for nominally zero-momentum spacecraft,[9] they are not readily useful for magnetic precession of bias momentum spacecraft because the precession torque persistently excites high-frequency nutations that, if not damped, ultimately cause chattering of the pitch dipole. Therefore, a bang-bang magnetic precession controller must be accompanied with a nutation damper. With regard to nutation damping, the superiority of an active scheme over passive for dual-spin spacecraft, using nutation rate feedback and coupling of the pitch controller with the roll/yaw motion through the roll/pitch or yaw/pitch product-of-inertia, is well known.[11] Consequently, a closed-loop bang-bang magnetic precession controller, working along with an active nutation controller, for bias momentum spacecraft in elliptic orbit is eminently suitable here and is shown in Fig. 7. The operation of this dual controller is essentially self-evident but its special features—the two deadbands and active nutation damping—are explained below. Also, $\boldsymbol{I}$ in Fig. 7 is the spacecraft's central inertia dyadic.

Magnetic Precession Controller

The polarity of the pitch dipole is now determined according to the bang-bang control law[9]

$$M_{m2} = |M_{m2}|\text{sgn}(\Delta \boldsymbol{h} \times \boldsymbol{B})_{y\text{-component}} \tag{39}$$

where $\Delta \boldsymbol{h}$, the excess angular momentum obtained from Eq. (23), is

$$\Delta \boldsymbol{h}^{\mathcal{F}^o} = h_s[-\alpha_3 \quad 0 \quad \alpha_1]^T \tag{40}$$

Substituting Eqs. (40) and (5) (wherein $\hat{\mu}_m$ and $\omega_0 t$ for circular orbit are replaced with μ_m/r^3 and true anomaly η, respectively, for elliptic orbit) in the law (39), it can be shown that

$$M_{m2} = |M_{m2}|\text{sgn}\{(\mu_m/r^3)h_s \sin\xi_m \times [\alpha_1 \cos(\eta - \eta_m) + 2\alpha_3 \sin(\eta - \eta_m)]\} \tag{41}$$

The strength $|M_{m2}|$ of the pitch dipole is set to be slightly larger than the mean strength $\bar{M}_{m2}$ [Eq. (38)]. The circular deadband in Fig. 7 precludes the use of the dipole when $A_\alpha \le A_{\alpha,\text{off}} = (\alpha_{1,\text{db}}^2 + \alpha_{3,\text{db}}^2)^{1/2}$ even if the magnetic field is strong; here, $A_{\alpha,\text{off}}$ is the maximum tolerable angle of deviation of the momentum vector $\boldsymbol{h}_s$ from the orbit normal, and $\alpha_{1,\text{db}}$ and $\alpha_{3,\text{db}}$(db = deadband) are the tolerable roll/yaw errors. If this inequality is not satisfied, the pitch dipole is turned on only if the surrounding magnetic field is strong enough to produce a substantial torque, that is, only if the spacecraft is at lower altitudes of the elliptic orbit. Quantitatively, if r_{weak} is the orbit radius beyond which the geomagnetic field is considered too feeble to be effective, Eq. (41) then suggests a deadband Δ_{hb} (see Fig. 7) equal to $\Delta_{\text{hb}} = (\mu_m/r_{\text{weak}}^3)|h_s|A_{\alpha,\text{off}} \sin i$, where the orbit inclination i is used because, for untilted geomagnetic dipole model, $\xi_m = i$. The pitch dipole is turned on with proper polarity if the argument of the sign function in Eq. (41) exceeds the deadband Δ_{hb}. The pitch dipole then generates roll and yaw control torques g_{b1} and g_{b3} according to Eq. (4).

Active Nutation Damping

The active nutation controller designed here does not use nutation rate feedback as in Ref. 11. Rather, it appears adequate to couple the roll/yaw motion with the pitch motion through a roll/pitch product of inertia and then damp the nutations through a standard PID pitch controller, as shown in Fig. 7. To accomplish this, Ref. 2 develops, using a root perturbation technique, the following parametric relationship between the desired nutation damping coefficient ζ_n and the required roll/pitch product of inertia I_{12}:

$$\zeta_n \Omega_n' = r_{\text{in}} K_D/[2I_2(1 - r_{\text{in}})] \tag{42}$$

where r_{in} is a nondimensional measure of the roll/pitch product-of-inertia I_{12} and Ω_n' is the nutation frequency of the spacecraft with a nonzero r_{in}, compared with the nutation frequency Ω_n for zero product-of-inertia:

$$r_{\text{in}} = I_{12}^2/(I_1 I_2) < 1 \tag{43}$$

$$\Omega_n' = \Omega_n(1 - r_{\text{in}})^{-\frac{1}{2}} \tag{44}$$

$$\Omega_n = |h_s|/\sqrt{I_1 I_3} \tag{45}$$

In Eqs. (42–45) I_1, I_2, I_3 are the roll, pitch, and yaw moments of inertia, respectively, of the spacecraft. In Eq. (42), K_D is the derivative gain of the PID pitch controller:

$$K_D = I_2(2\zeta\omega_{\text{bw}} + \lambda) \tag{46}$$

$$\lambda = 5\zeta\omega_{\text{bw}} \tag{47}$$

ω_{bw} being the bandwidth, ζ the damping coefficient (0.707, typically), and $-\lambda$ the real root of the pitch controller. For the specified parameters ζ_n, Ω_n, K_D and the pitch inertia I_2, Eq. (42) specifies the required product-of-inertia parameter r_{in}. It is reassuring to note that the nutation damping time constant [Eq. (14)][11] for dual-spin spacecraft reduces to $\zeta_n \Omega_n'$ [Eq. (42)] when, in the former equation, the gain K_D and the phase (−90 deg) of the pitch controller at the frequency Ω_n' are substituted.

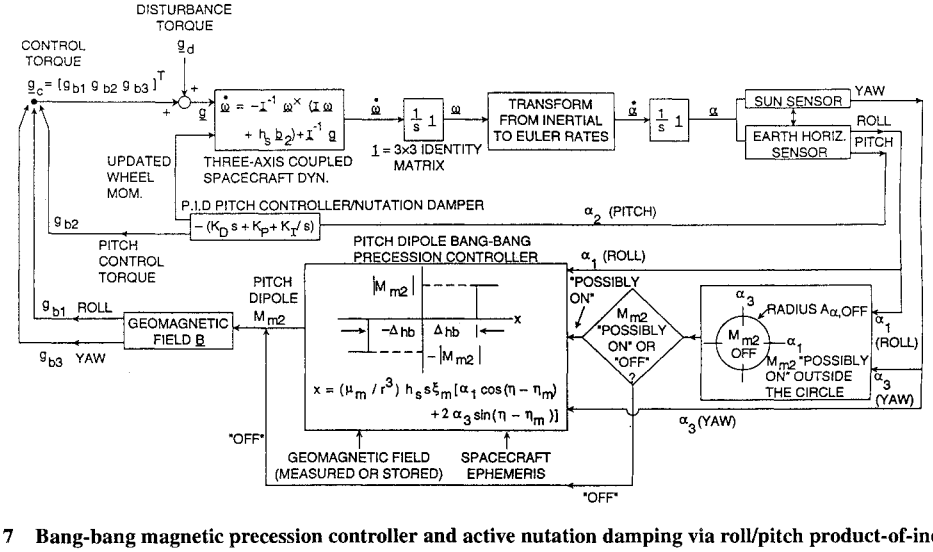

Fig. 7 Bang-bang magnetic precession controller and active nutation damping via roll/pitch product-of-inertia.

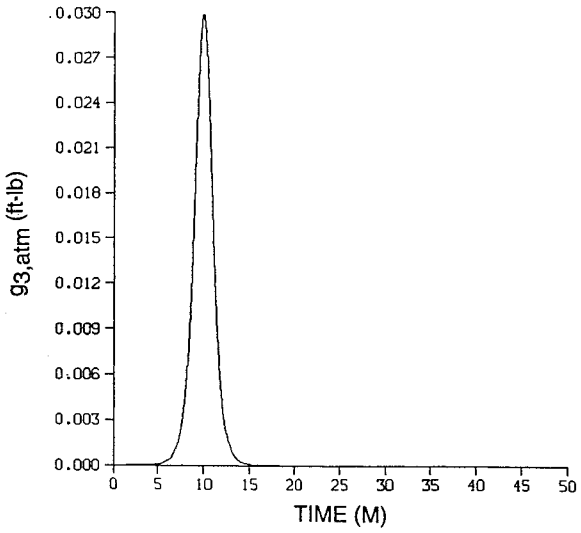

Fig. 8 Yaw atmospheric torque near perigee.

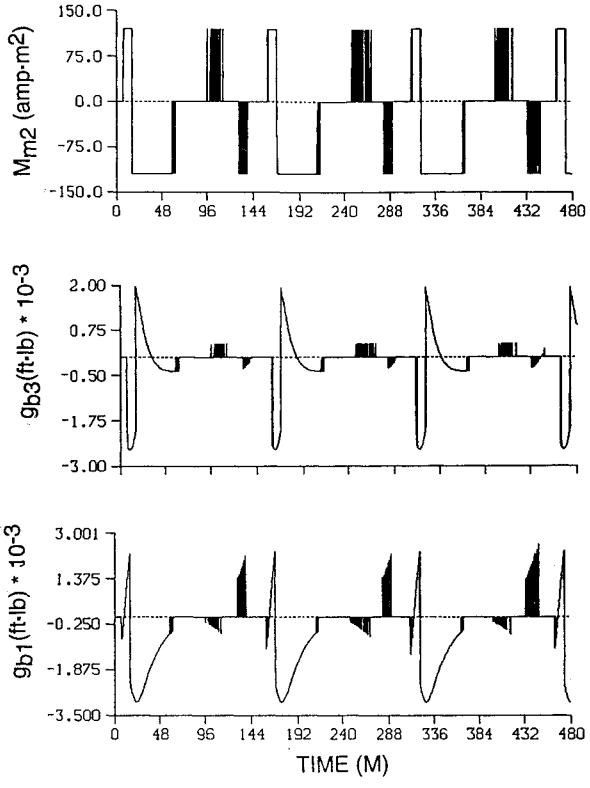

Fig. 9 Roll and yaw magnetic torques (g_{b1}, g_{b3}) and pitch dipole (M_{m2}) vs time.

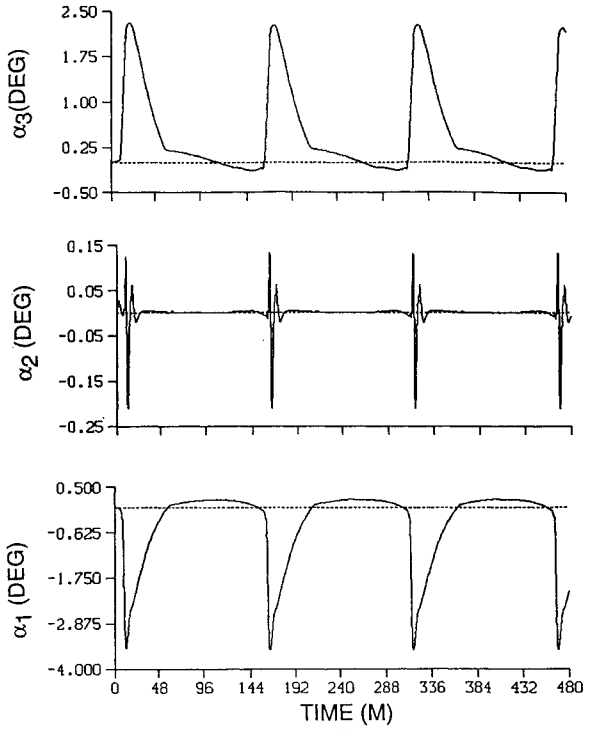

Fig. 10 Roll, pitch, and yaw angles vs time.

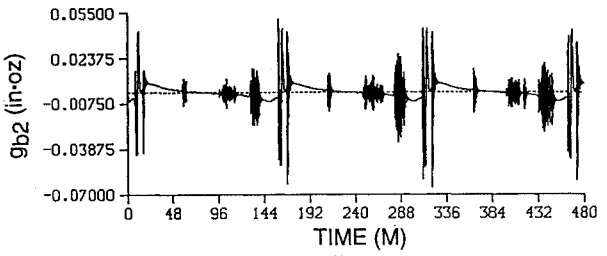

Fig. 11 Momentum wheel torque about pitch axis vs time.

Illustration

Consider a small spacecraft designed for aeronomy traversing an elliptic orbit. Its relevant parameters are recorded in Table 2 except h_s, which is now -81.35 N · m · s; the following additional parameters also apply:

$$I_1, I_2, I_3 = 81.78, 76.09, 60.25 \text{ kg} \cdot \text{m}^2 \qquad r_{\text{in}} = 0.3469$$

$$\omega_{\text{bw}}/\omega_0 = 16, \zeta = 0.707 \qquad I_{12} = 46.46 \text{ kg} \cdot \text{m}^2$$

$$\Omega_n/\omega_0 = 1682.68 \qquad \Omega_n'/\omega_0 = 2082.66$$

$$\Omega_n/\omega_{\text{bw}} = 105.16 \qquad 2\pi/\Omega_n' = 4.38 \text{ s} \quad \text{(nutation period)} \quad (48)$$

where r_{in} and I_{12} correspond to the nutation damping coefficient $\zeta_n = 0.01$. Reflecting on the values of Ω_n/ω_0, $\Omega_n/\omega_{\text{bw}}$, and $\omega_{\text{bw}}/\omega_0$, the assumptions in the analysis that the wheel angular momentum is far greater than the satellite's own momentum and the nutation frequency is much greater than the pitch controller frequency are both justified. The sample period for the pitch controller is selected to be 0.25 s and that for the precession controller is set at 1 s. Because of low perigee altitude (120 km), the spacecraft experiences a significant atmospheric torque near perigee, shown in Fig. 8, where $t = 0$ corresponds to the true anomaly $\eta = -45$ deg. Since the orbital period is 152 min, this repetitive torque is quasi-impulsive, and the performance of the above controller over 480 min (more than three orbits) is shown in Figs. 9–12.

The amplitude $A_{\alpha,\text{off}}$ is set at 0.2 deg, and the orbit radius r_{weak} corresponds to the true anomaly $\eta = \pm 135$ deg; the deadband Δ_{hb} is calculated accordingly. The roll and yaw magnetic control torque and the corresponding bang-bang profile of the pitch dipole with some high-frequency switching are shown in Fig. 9. The positive yaw atmospheric torque (Fig. 8) produces a significant negative roll precession in the beginning (Fig. 10), which in turn activates both the bang-bang magnetic controller (Fig. 9) and the PID pitch controller (Fig. 11). Subsequent motion is very coupled and it is clear from Fig. 9 that the magnets are on for long periods (60 min approximately) and turned off after nearly 65 min when the deadband conditions are satisfied. After approximately $t = 100$ min, the magnets are turned on and off several times relatively rapidly near the $A_{\alpha,\text{off}}$ circle, and the nutations that are caused by the magnets are well damped by the speed modulation of the wheel, governed by the PID controller (Fig. 11). Figure 12 exhibits well-damped rate profiles, with a time constant of $1/\zeta_n\Omega_n = 1.16$ min. The attitude and rate determination aspect of the above scheme is sketched in Ref. 2.

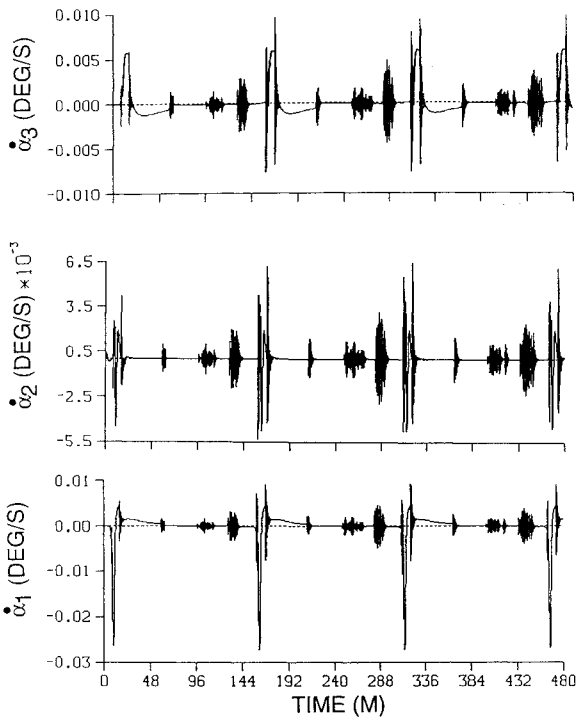

Fig. 12 Roll, pitch, and yaw Euler rates vs time.

VI. Concluding Remarks

The general sizing equation for a pitch dipole developed in the preceding for π radian yaw precession of bias momentum satellites in circular orbits is useful for quick studies. Such yaw precessions, however, are inevitably accompanied with high-frequency nutations and substantial roll motion, both within linear range. After completing the yaw precession, these undesired motions can be eliminated using a linear magnetic controller. Moreover, the Earth-pointing rate about the pitch axis, halted before commencing the precession, must be reestablished after precession, and any large deviation from the Earth-pointing attitude must be corrected for by modulating the pitch momentum wheel speed. For elliptic orbits, the pitch dipole sizing equation for small angle roll/yaw precession is useful for determining the strength (in ampere · meter^2) required for a closed-loop, bang-bang magnetic precession. One such closed-loop controller, working together with nutation damping via a roll/pitch product-of-inertia and a pitch controller, and its performance under periodic, nearly impulsive, atmospheric torque around the perigee is presented. In a continuation of this study but not reported here due to space limitations, the performance of this controller is found to be very satisfactory even under realistic noisy measurements from horizon sensors and sun sensors.

References

[1]Bollner, M., Pietrass, A., and Stapf, R., "Spin Axis Magnetic Coil Maneuvers of the AMPTE/IRM Spacecraft," *Proceedings of the AIAA Guidance, Navigation, and Control Conference*, AIAA, New York, 1985, pp. 508–517.

[2]Hablani, H. B., "Magnetic Precession and Product-of-Inertia Nutation Damping of Bias Momentum Satellites," *Proceedings of the AIAA Guidance, Navigation, and Control Conference* (Scottsdale, AZ), AIAA, Washington, DC, 1994, pp. 154–169.

[3]Shigehara, M., "Geomagnetic Attitude Control of an Axisymmetric Spinning Satellite," *Journal of Spacecraft and Rockets*, Vol. 9, No. 6, 1972, pp. 391–398.

[4]Woolley, R. D., and Werking, R. D., "Computer Simulation for Time Optimal or Energy Optimal Attitude Control of Spin-Stabilized Spacecraft," *Proceedings of Summer Computer Simulation Conference, Montreal, Canada*, Vol. 1, Society for Computer Simulation, La Jolla, CA, 1973, pp. 448–453.

[5]Junkins, J. L., Carrington, C. K., and Williams, C. E., "Time-Optimal Magnetic Attitude Maneuvers," *Journal of Guidance and Control*, Vol. 4, No. 4, 1981, pp. 363–368.

[6]Rajaram, S., and Goel, P. S., "Magnetic Attitude Control of Near Earth Spinning Satellites," *Journal of the British Interplanetary Society*, Vol. 31, 1978, pp. 163–167.

[7]McElvain, R. J., "Satellite Angular Momentum Removal Utilizing the Earth's Magnetic Field," *Torques and Attitude Sensing in Earth Satellites*, edited by S. F. Singer, Academic, New York, 1964, pp. 137–158.

[8]Lebsock, K., and Eterno, J., "Design of a Maneuverable Momentum Bias Attitude Control System," *Proceedings of AIAA/AAS Astrodynamics Conference* (Minneapolis, MN), AIAA, Washington, DC, 1988, pp. 704–713.

[9]Camillo, P. J., and Markley, F. L., "Orbit-Averaged Behavior of Magnetic Control Laws for Momentum Unloading," *Journal of Guidance and Control*, Vol. 3, No. 6, 1980, pp. 563–568.

[10]Hablani, H. B., "Comparative Stability Analyses and Performance of Magnetic Controllers for Momentum Bias Satellites," *Proceedings of the American Astronautical Society/Goddard Space Flight Center International Symposium on Space Flight Dynamics*, Greenbelt, MD, 1993, pp. 1–18 (AAS Paper 93-278).

[11]Smay, J. W., and Slafer, L. I., "Dual-Spin Spacecraft Stabilization Using Nutation Feedback and Inertia Coupling," *Journal of Spacecraft and Rockets*, Vol. 13, No. 11, 1976, pp. 650–659.